Journal of Alloys and Compounds 724 (2017) 98–102

Contents lists available at ScienceDirect

Journal of Alloys and Compounds

journal homepage: http://www.elsevier.com/locate/jalcom

Temperature effects on the structural and optical properties of the $TlInSe_{2x}S_{2(1-x)}$ mixed crystals ($x = 0.3$)

A. Omar [a], A.F. Qasrawi [a, b, *], N.M. Gasanly [c]

[a] Department of Physics at Arab American University, Jenin, Palestine
[b] Group of Physics, Faculty of Engineering, Atilim University, 06836, Ankara, Turkey
[c] Physics Department, Middle East Technical University, 06800, Ankara, Turkey

ARTICLE INFO

Article history:
Received 19 January 2017
Received in revised form
9 June 2017
Accepted 30 June 2017
Available online 1 July 2017

Keywords:
Deformation
Defects in solids
Optical properties
Smart materials

ABSTRACT

In this work, we have studied the temperature effects on the recrystallization process and on the energy band gap of the $TlInSe_{2x}S_{2(1-x)}$ mixed crystals at the critical composition ($x = 0.3$) where structural phase transition from tetragonal to monoclinic takes place. Remarkable effect which included permanent recrystallization process, enlargements in the monoclinic crystallite size, decreases in the compressing strain and in the dislocation density as well as in the stacking faults and in the energy band gap with increasing temperature were observed. In addition, the temperature dependent energy band gap of the crystal which is investigated in the same temperature range that was used for the recrystallization process revealed that the recrystallization process is associated with energy band gap narrowing.

© 2017 Elsevier B.V. All rights reserved.

1. Introduction

The $TlInS_2$ and $TlInSe_2$ based mixed crystals have been attracting the attention of research society since more than 20 years. The importance of these two crystals arises from their applicability in the nonlinear two - photon processes. These anharmonic optical dynamics which are observed in thallium chalcogenides [1] can provide substantial contribution to the nonlinear optical effects of the third order. The two-photon processes are sensitive to the temperature excited additional phonon contributions. In addition, the $TlInS_2$ and $TlInSe_2$ based mixed crystals gain interest as they can be used as electron paramagnetic resonator when doped with Fe^{3+} [2], as current controlled memory devices [3] and as photovoltaics [4,5]. The mixed crystals which are composed of these two materials are reported to exhibits interesting structural, optical and electrical properties. As for example, the TlInSeS compound exhibit monoclinic structure with direct and indirect band gaps of 2.05 and 2.21 eV, respectively [6,7]. It was also observed that the energy band gap of the $TlInS_{2x}Se_{2(1-x)}$ mixed crystals ($0.25 \leq x \leq 1$) decreases with the increase of selenium atoms content [8]. Such property provides wide variety in the optoelectronic properties of these materials.

The switching phenomena, memory effect and negative resistance behavior in the TlInSeS are reported to be sensitive to the temperature, crystal thickness and illumination intensity [9]. In addition, the temperature is also observed to play vital role on the performance of the Si doped $TlInSe_2$–$TlInS_2$ mixed crystals ($Tl_{1-x}In_{1-x}Si_xSe_2$). Particularly, the temperature strongly influenced the electroconductivity and photoinduced absorption at 0.15 eV [10]. The temperature is also mentioned as a controller of the impurity behavior of these mixed crystals.

The $TlInS_2$, for example, exhibits microwave dielectric dispersion associated with structural modifications. Such types of crystals show strongly overdamped soft ferroelectric modes. The frequency of these modes drops to the millimeter wave region causing dielectric microwave dispersion and increases the static dielectric permittivity. As the defects and impurities leads to the pinning of the soft mode, the dynamical dielectric properties are significantly altered [11]. In addition, the intrinsic defects which are presented in these layered crystals are accepted to be a source of a huge number of trapping levels below the top of energy gap. The formation of the sub-bands by such intrinsic defect's affect the scattering mechanisms of the charge carriers and phonons [1]. Thus, they results in substantially narrowing the actual energy band gap.

The above mentioned attenuations in the physical properties via

* Corresponding author. Department of Physics at Arab American University, Jenin, Palestine.
E-mail addresses: atef.qasrawi@atilim.edu.tr, atef.qasrawi@aauj.edu (A.F. Qasrawi).

http://dx.doi.org/10.1016/j.jallcom.2017.06.337
0925-8388/© 2017 Elsevier B.V. All rights reserved.

temperature variations motivated us to explore the temperature effects on the microstructure of the $TlInSe_{2x}S_{2(1-x)}$ mixed crystals ($x = 0.3$). Particularly, the temperature effects on the micro strain, lattice constants, dislocation density, crystallite size and degree of orientation are studied in the temperature range of 300–450 K using the X-ray diffraction technique. In addition, the relation of these structural modifications to the temperature dependence of the energy band gap is investigated.

2. Experimental details

$TlInSe_{0.6}S_{1.4}$ polycrystals prepared from high-purity elements (at least 99.999%) taken in stoichiometric proportions. $TlInSe_{0.6}S_{1.4}$ single crystals were grown by the Bridgman method in evacuated (10^{-5} Torr) silica tubes with a tip at the bottom. The ampoule was moved in a vertical furnace through a thermal gradient of 30 °Ccm^{-1}, between the temperatures 780 and 430 °C at a rate of 1.0 mmh^{-1}. The resulting ingots (orange in color) showed good optical quality and the freshly cleaved surfaces were mirror-like. A sample with 5.0 mm × 7.0 mm × 1.9 mm dimensions was used for the measurements.

The temperature dependent X-ray diffraction patterns were recorded in the temperature range of 300–470 K, using temperature exchanger attached to the Rigaku miniflex-600 X-ray unit. The scanning speed was 0.05 deg./s. On the other hand, the optical properties were recorded with the help of Thermoscientific Evolution 300 spectrophotometer equipped with VEE-Max III reflectometer.

3. Results and discussion

Depending on the published data [12] about the $TlInSe_{2x}S_{2(1-x)}$ mixed crystals which indicate that the mixed crystals exhibit structural phase transitions from the tetragonal $TlInSe_2$ to the monoclinic $TlInS_2$ at a content (x) of 0.30, we have carried out detailed temperature-dependent structural analysis on this mixed crystal ($TlInSe_{0.6}S_{1.4}$). The resulting X-ray powder diffraction (XRD) data of the $TlInSe_{0.6}S_{1.4}$ mixed crystal in the temperature range of 30–200 °C are shown in Fig. 1. The figure indicates well crystalline phase of the material. In order to understand, the properties of this phase, the resulting XRD patterns were subjected to software analysis using the "TREOR 92" and "Crystdiff " software packages. The analysis of the nine observed peaks (Fig. 1) had shown that the crystal exhibits tetragonal unit cell characteristics with lattice

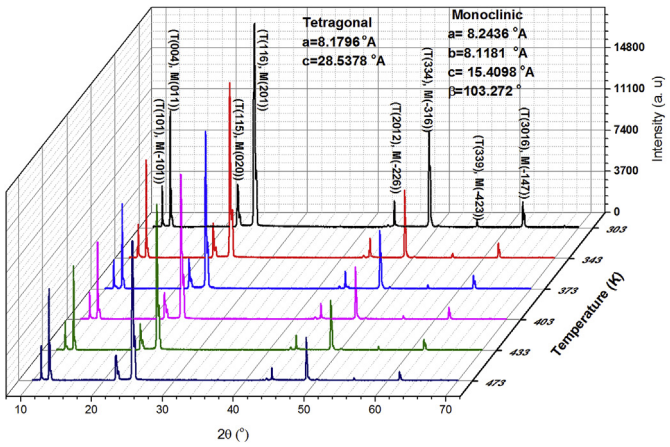

Fig. 1. The temperature dependent X-ray diffraction patterns of the $TlInSe_{0.6}S_{1.4}$ crystals.

parameters of a= 8.1799 and c= 28.5378 °A at temperature of 303 K. The most strong reflection peak which appeared at $2\theta = 24.247^{\circ}$ is in the (116) direction. The second less strong peak which appeared at $2\theta = 12.4075^{\circ}$ occurs in the (115) orientation direction. The difference between the measured and calculated 2θ values was mostly 0.024 and for one minor peak ($2\theta = 55.69^{\circ}$) it was 0.068 at maximum. With these restrictions, the tetragonal structural phase with the mentioned lattice parameters appears to fit well with the properties of the $TlInSe_{2x}S_{2(1-x)}$ before the structural transition from tetragonal to monoclinic taking place. The calculated lattice parameters for the tetragonal unit cell are comparable to those reported for $\beta-$ $TlInS_2$ as a = 7.680 Å and c = 29.976 Å which relate to the space group $I4/mcm$ comprising 16 formula units [13]. The values are very different from those reported for the tetragonal $TlInSe_2$ as a = 8.071 and c = 6.861 Å [13,14]. On the other hand, the experimental data revealed an exact solution for a monoclinic unit cell of lattice parameters of a = 8.2436 Å, b = 8.1181 Å, c = 15.4098 Å and $\beta = 103.72$ °. The maximum peak orientation appears in the (201) direction. The difference between the observed and calculated 2θ values for this unit cell was mostly 0.003 (including the peak observed at $2\theta = 55.69^{\circ}$) and reaches 0.024 at most for two minor peaks. The lattice parameters values for the monoclinic unit cell are less than those reported for $TlInS_2$ crystals [13]. They are also different from those reported for the monoclinic TlInSeS crystals as a = 0.72850, b = 0.45380, c = 0.78357 nm, and β = 106.22° [15]. The reason beyond these differences should be assigned to the S and Se atomic compositions. The $TlInS_2$ and $TlInSe_2$ crystal systems are reported to exhibit low-dimensional structures with the crystal lattice being composed of alternating two dimensional layers oriented parallel to the (001) plane [8]. Each successive layer is rotated by 90° with respect to the previous layer. The bonding of the interlayers and intralayers are formed between the Tl and S, and In and S atoms, respectively. This bonding mechanism forces the Tl atoms to follow chain order along the [110] and [110^{-}] directions [8]. In addition, in the $TlInSe_2$ crystal, the univalent Tl and trivalent In atoms exists in a tetrahedral Se environment, thus, the $InSe_4$ tetrahedral of the unit cell form chains parallel to the c-axis extending along the [001] directions. Such chains are bonded with each other by Tl atoms. As mentioned at the beginning of this section, the transformation from tetragonal to monoclinic should have taken place at $x = 0.3$. So with critical composition, the solution of the X-ray diffraction patterns likely to be of monoclinic type owing to the more close values of the calculated diffraction angles to those observed in Fig. 1.

The effect of temperature on the crystallization process, which is studied in the temperature range of 303–473 K and shown in Fig. 1, is better presented in Fig. 2. The figure shows the enlargement of the maximum peak as a function of temperature. As seen, the peaks systematically shift toward lower 2θ values. The shift is associated with a decrease in the XRD patterns intensity (inset of Fig. 2). This systematic shift is an indication of uniform deformation or recrystallization. The recrystallization is defined as the formation of new, strain-free, equiaxed grains from previously strain-hardened grains. In the recrystallization process, the deformed grains are replaced by a new set of undeformed grains that nucleate and grow until the original grains have been entirely consumed. When the XRD patterns were recorded after the sample was cooled to room temperature, the X-ray diffraction patterns were the same as those which was recorded at 473 K indicating that the deformation (recrystallization) is of an inelastic type. The same conclusion is valid for any other temperature cycling. As another example, when the sample was heated at 373 K and then cooled to room temperature, the X-ray diffraction patterns at room temperature are like those which were observed at 373 K. The structural deformations

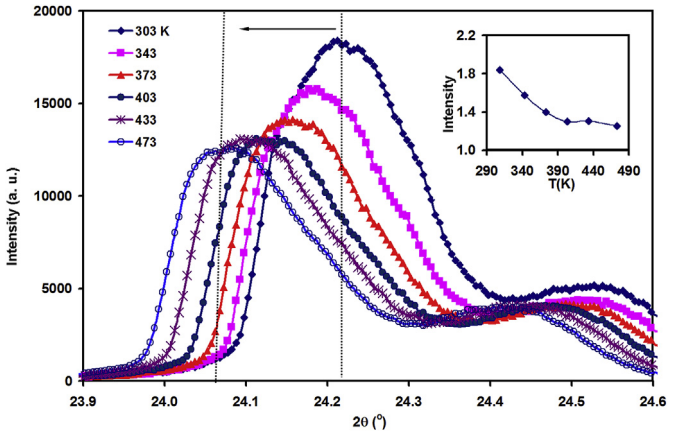

Fig. 2. Enlargement of the most intensive peak in the XRD patterns of the $TlInSe_{0.6}S_{1.4}$ crystals showing the deformation effects. The inset shows the decrease in the peak intensity as function of temperature.

(recrystallization) are permanent. The XRD patterns were also recorded at room temperature three weeks later and no change in the patterns were observed. To understand the reasons for this permanent deformation (recrystallization) which resulted from temperature variation, the crystallite size (D), microstrain ($\in$), dislocation (defect) density (δ) and stacking faults (SF) were calculated from the broadening width (β) of the most intensive peak with the help of the equations, $D = 0.94\lambda/(\beta\cos(\theta))$, $\varepsilon = \beta/(4\tan(\theta))$, $\delta = 15\in/(aD)$ and $SF = \frac{2\pi^2\beta}{(45\sqrt{3}\tan(\theta))}$ [16,17], respectively. The respective temperature-dependent calculations are shown in Fig. 3 (a)-(d). As seen from Fig. 3 (a) an increase in the crystallite size from 43.5 to 47.5 nm is associated with temperature increase from 303 to 473 K. Consistently, the strain (Fig. 3 (b)) decreases with increasing temperature indicating that there exist an atomic displacement. The decrease in the compressing strain with temperature should be a significant reason for the enhancement of the crystallite size with temperature. In like manner, the defect density (Fig. 3 (c)) and the stacking faults (ST) also systematically decrease by ~ 13–15% of the original value. All the parameters are consistently varying indicating that the $TlInSe_{0.6}S_{1.4}$ exhibits systematic recrystallization upon heating up to 473 K.

Similar studies concerned the increase in the crystallite size, the decrease in stacking faults, the decrease in microstrain and in the defect density with increasing substrate temperature of MoO_3 films [17]. These studies concluded an enhanced recrystallization process through temperature variation. This response to temperature variation in MoO_3 films was assigned to the formation of microplates that result from the aggregation or fusion of small particles at higher temperatures [17]. The increase in the crystallite size with increasing temperature was also observed for the $AgIn_5S_8$ polycrystalline films [18]. This behavior was assigned to the reduction in the internal energy. The crystallite growth happens when recovery and recrystallization processes are complete and no further reduction in the internal energy could be possible. For this reason, the total energy stabilization can be achieved by reducing the total area of the crystallite boundaries. In recovery process, the deformed crystallites may reduce their stored energy by the removal or rearrangement of defects in their crystal structure which also explains the behavior of Fig. 3 (c) and (d). Consistently, during the recrystallization process, the deformed crystallites are replaced by a new set of unreformed crystallites that nucleate and grow until the original crystallites have been entirely consumed [18,19].

The increase in the crystallite size that is associated with lower defect density and decreasing stacking faults play vital role in the optical and electronic performance of the $TlInSe_{2x}S_{2(1-x)}$ crystals. The earlier studies have shown that band gap energy in the temperature region of 10–300 K, decreases with increasing temperature in accordance with the equation,

$$E_g(T) = E_g(0) + \gamma T^2 \Big/ (\theta_D + T) \quad (1)$$

with $\gamma = dE_g/dT$ being the temperature gradient of the band gap

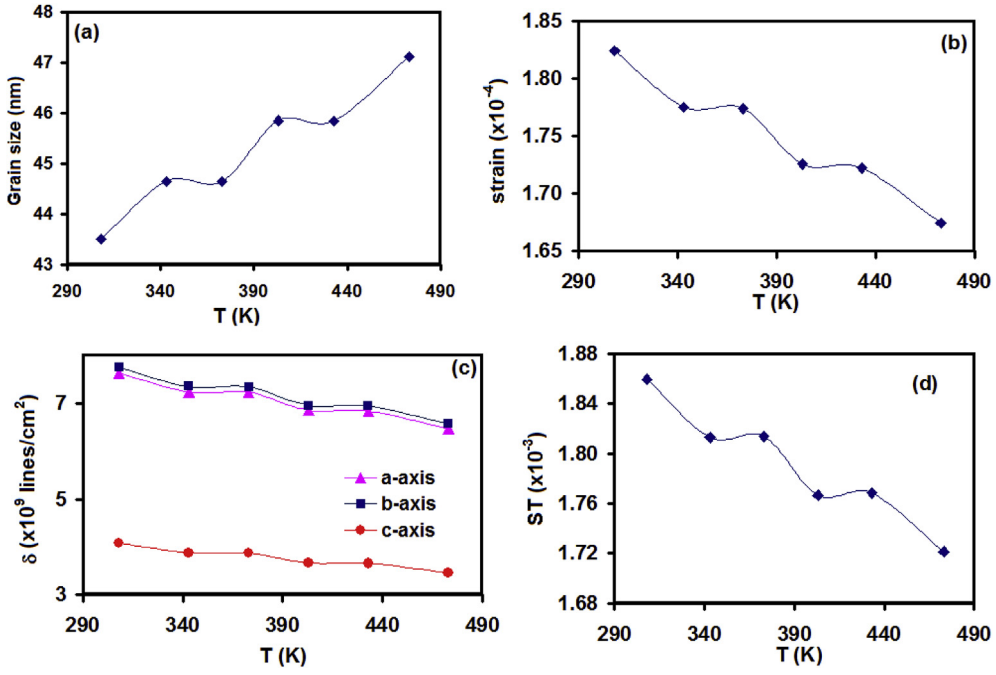

Fig. 3. The temperature dependent (a) crystallite size, (b) strain, (c) defect density and (d) stacking faults for the $TlInSe_{0.6}S_{1.4}$ crystals.

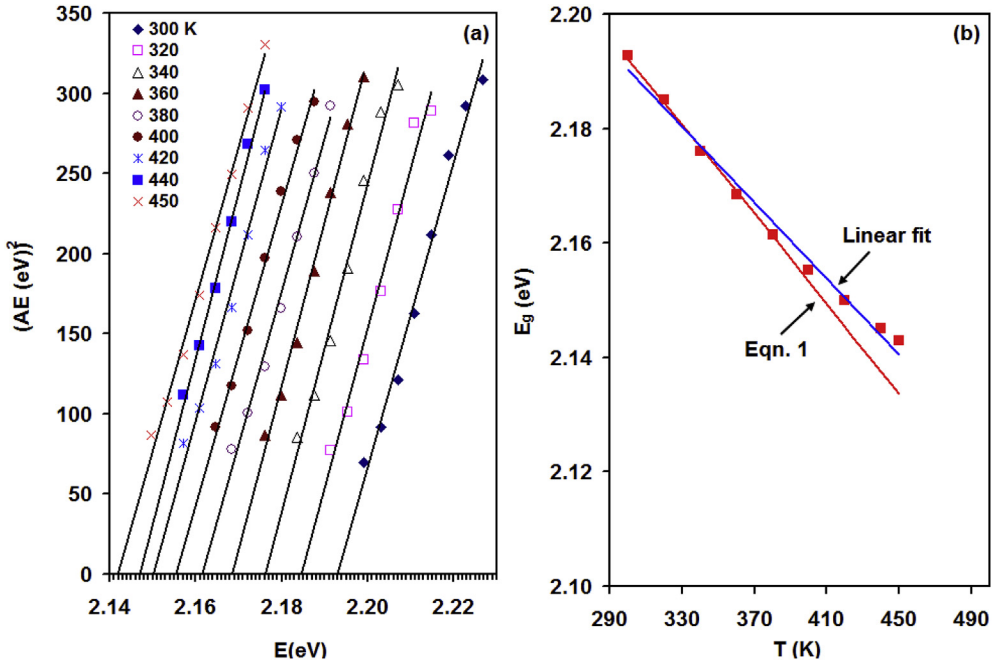

Fig. 4. The temperature dependent (a) $(\alpha E)^2 - E$ variation and (b) energy band gap.

and θ_D being the Debye temperature [8]. To observe the effects of the structural modifications on the energy band gap we have recoded the optical absorbance (A) as function of temperature in the range of 303–473 K. The calculation of the energy band gap is determined from Tauc equation, $(AE)^2 = (E - E_g)$, which is presented in Fig. 4 (a) [8]. The $E - axis$ crossings which are shown by the solid lines in Fig. 4 (a) allowed determining the energy band gap values as function of temperature. As illustrated in Fig. 4 (b), the energy band gap decreases with increasing temperature as expected. The fitting of Eqn. (1), which is shown by solid line in Fig. 4 (b), reveals the value of $\gamma = -4.2 \times 10^{-4}\ eV/K$, $E_g(0) = 2.28\ eV$ and $\theta_D = 135\ K$. These parameters are consistent with those reported for $TlInSe_{0.5}S_{1.5}$ crystals [8]. Due to the narrow range of temperature, the fitting of the experimental data of the $E_g - T$ dependence with Eqn. (1) could be of less physical significance, thus, the $E_g - T$ variation could also be approximated by linear fitting through the equation, $E_g(T) = -\gamma T + E_g(0)$. In this case the values of γ and $E_g(0)$ are found to be $-3.3 \times 10^{-4}\ eV/K$ and 2.29 eV, respectively. The values of γ and $E_g(0)$ which are evaluated by Eqn. (1) and by the linear fitting are comparable to each other indicating the same sensitivity to temperature variations. The shrinkage in the energy band gap value as a result of temperature raising is assigned to the enlargement of the crystallite size that is associated with compressing strain and less stacking faults. In other words, as the temperature increases, the lattice constant decreases (compressing strain) causing a relaxation of the residual stress. Stresses result from the existence of vacancies and interstitial atoms [20]. Numerical simulations have shown that the stacking fault energy result in low vacancy production and the high stacking fault energy results in collective reactions of complete lattice dislocations and the accumulation of high vacancy concentrations [21]. While the vacancy destroys the balance of attraction and repulsion between neighboring crystal planes leading to the contraction of the crystal lattice and the existence of tensile stress, the interstitial atoms at the normal sites of the lattice excludes each other leading to the expansion of lattice parameters and hence causing compressive stress [20]. Since the lattice constant is related to the uniform strain and biaxial stress along a particular axis, the dominant tensile strain increases the grain size with increasing temperature. It is also believed that with the raising of the temperature, the residual stress relaxes and the tensile strain dominates. Similar studies on doped ZnO thin films assigned the narrowing in the energy band gap with increasing temperature to the increase in the grain size and decrease in the compressing strain. They attributed the shrinkage in the band gap to the domination of the tensile strain [20]. In addition, the temperature-dependent recrystallization process enhances activated population of phonon in the $TlInSe_{0.6}S_{1.4}$ crystals, which in turn causes more electron-phonon interaction. This interaction also results in band gap shrinkage at high temperatures [22]. In addition, in accordance with Eqn. (1), the amplitude of atomic vibrations increases with increasing temperature leading to larger interatomic spacing and forcing stronger lattice phonon excitations as well. The interaction between the lattice phonons and the free electrons and holes also affects the band gap. Such kind of crystals which exhibit a shrinking in the energy band gap upon heat treatments are of particular interest for the photoinduced laser operation. They are extremely important when using them as infrared materials operating at ambient conditions [23].

4. Conclusions

In the current work, we have investigated the temperature effects on the recrystallization process as well as the crystallite size, strain, dislocation density, stacking faults and energy band gap of the $TlInSe_{2x}S_{2(1-x)}$ ($x = 0.3$) at the structural phase transition point from tetragonal to monoclinic. It was observed that the increase in the temperature causes better permanent recrystallization associated with a decrease in the energy band gap value with increasing temperature. The shrinkage in the energy band gap as a result of temperature recrystallization process of the $TlInSe_{2x}S_{2(1-x)}$ crystals makes it more appropriate for use as an active media for photoinduced laser operations.

Acknowledgments

This project was funded by the Deanship of Scientific Research (DSR), at Arab American University, Jenin, under the grant number Cycle I 2016–2017. The authors, therefore, acknowledge with thanking the DSR technical and financial support.

References

[1] G.E. Davydyuk, M. Piasecki, O.V. Parasyuk, G.L. Myronchuk, A.O. Fedorchuk, S.P. Danylchuk, L.V. Piskach, M. Yu Mozolyuk, N. AlZayed, I.V. Kityk, Two-photon absorption of Tl 1– xIn 1– xSnxSe 2 (x= 0, 0.1, 0.2, 0.25) single crystalline alloys and their nanocrystallites, Opt. Mater. 35 (12) (2013) 2514–2518.

[2] F. Mikailzade, M. Maksutoglu, R.I. Khaibullin, V.F. Valeev, V.I. Nuzhdin, V.B. Aliyeva, T.G. Mammadov, Magnetodielectric effects in Co-implanted $TlInS_2$ and $TlGaSe_2$ crystals, Phase Trans. 89 (6) (2016) 568–577.

[3] A.T. Nagat, S.A. Hussien, A.A. Ebnalwaled, S.R. Alharbi, S.E. AlGarni, L.A. Alkahtani, Current controlled negative resistance with memory in some binary thallium chalcogenide semiconductor compound, J. Mechatron. 3 (4) (2016) 322–330.

[4] K. Wakita, Y. Araki, R. Asaba, Y. Shim, N. Mamedov, Photoluminescence spectra of $TlInSe_2$, Phys. Status Solidi (c) 9 (12) (2012) 2352–2354.

[5] A. P Odrinskii, M.H. Yu Seyidov, R.A. Suleymanov, T.G. Mammadov, V.B. Aliyeva, Photovoltaic currents and activity of structural defects in a ferroelectric–semiconductor $TlInS_2$: La single crystal, Phys. Solid State 58 (4) (2016) 716–722.

[6] S. Hosokawa, K. Kamimura, H. Ikemoto, N. Happo, K. Mimura, K. Hayashi, K. Takahashi, K. Wakita, N. Mamedov, Structural studies on TlInSe2 thermoelectric material by X-ray fluorescence holography, XAFS, and X-ray diffraction, Phys. status solidi (b) 252 (6) (2015) 1225–1229.

[7] N.M. Gasanly, Temperature-tuned band gap energy and oscillator parameters of $Tl_2InGaSe_4$ semiconducting layered single crystals, Cryst. Res. Technol. 44 (3) (2009) 322–326.

[8] N.M. Gasanly, Effect of temperature and isomorphic atom substitution on optical absorption edge of $TlInS_{2x}Se_{2(1-x)}$ mixed crystals (0.25≤ x≤ 1), Cryst. Res. Technol. 45 (5) (2010) 525–528.

[9] S. Al Garni, Negative resistance and memory effects in TlInSeS single crystals, Jpn. J. Appl. Phys. 52 (11R) (2013) 115802.

[10] G.L. Myronchuk, O.V. Zamurueva, K. Oźga, M. Szota, A.M. El-Naggar, N.S. Alzayed, L.V. Piskach, O.V. Parasyuk, A.A. Albassam, A.O. Fedorchuk, I.V. Kityk, Photoinduced optical properties of $Tl_{1-x}In_{1-x}Si_xSe_2$ single crystals, Archives Metall. Mater. 60 (2) (2015) 1051–1055.

[11] J. Banys, A. Brilingas, J. Grigas, Pinning effect on microwave dielectric properties and soft mode in TlInS2 and $TlGaSe_2$ ferroelectrics, Phase Trans. A Multinatl. J. 20 (3–4) (1990) 211–229.

[12] E. Kerimova, S. Mustafaeva, D. Guseinova, I. Efendieva, S. Babaev, T.G. Mamedov, T.S. Mamedov, Z. Salaeva, K. Allakhverdiev, The influence of hydrostatic pressure on the electrical conductivity and optical properties of chain-layered $TlInSe_2$ and $TlInSe_2$–$TlInS_2$ solid solutions, Phys. status solidi (a) 179 (1) (2000) 199–203.

[13] D.I. Ismailov, Electron diffraction investigation of phase transitions in A3 B3 C2 6 compounds, Fizika 10 (2004) 29–39.

[14] A.F. Qasrawi, F.G. Aljammal, N.M. Taleb, N.M. Gasanly, Design and characterization of TlInSe2 varactor devices, Phys. B Condens. Matter 406 (14) (2011) 2740–2744.

[15] N.M. Gasanly, I. Guler, Temperature-tuned band gap energy and oscillator parameters of TlInSeS layered single crystals, Int. J. Mod. Phys. B 22 (22) (2008) 3931–3939.

[16] N.M. Khusayfan, S.E. Al Garni, A.F. Qasrawi, Design and performance of Yb/ZnS/C Schottky barriers, Curr. Appl. Phys. 17 (1) (2017) 115–119.

[17] M. Balaji, J. Chandrasekaran, M. Raja, Role of substrate temperature on MoO_3 thin films by the JNS pyrolysis technique for P–N junction diode application, Mater. Sci. Semicond. Process. 43 (2016) 104–113.

[18] A.F. Qasrawi, T.S. Kayed, F. Ercan, Heat treatment effects on the structural and electrical properties of thermally deposited $AgIn_5S_8$ thin films, Solid State Commun. 151 (8) (2011) 615–618.

[19] R.D. Doherty, D.A. Hughes, F.J. Humphreys, J.J. Jonas, D.J. Jensen, M.E. Kassner, W.E. King, T.R. McNelley, H.J. McQueen, A.D. Rollett, 1997, Current issues in recrystallization: a review, Mater. Sci. Eng. A 238 (2) (1997) 219–274.

[20] J.P. Mathew, G. Varghese, J. Mathew, Effect of doping concentration and annealing temperature on the structural and optical properties of Zn 1– x Cu x O films, SOP Trans. Nano-Technol. 1 (3) (2014) 1–11.

[21] V. Borovikov, M.I. Mendelev, A.H. King, R. Lesar, Effect of stacking fault energy on mechanism of plastic deformation in nanotwinned FCC metals, Model. Simul. Mater. Sci. Eng. 23 (5) (2015) 055003.

[22] P.K. Sarswat, L.F. Michael, A study of energy band gap versus temperature for Cu_2ZnSnS_4 thin films, Phys. B Condens. Matter 407 (1) (2012) 108–111.

[23] M. Piasecki, G.L. Myronchuk, O.V. Zamurueva, O.Y. Khyzhun, O.V. Parasyuk, A.O. Fedorchuk, A. Albassam, A.M. El-Naggar, I.V. Kityk, Huge operation by energy gap of novel narrow band gap Tl1– x In1– x B x Se2 (B= Si, Ge): DFT, x-ray emission and photoconductivity studies, Mater. Res. Express 3 (2) (2016) 025902.